

## Net-baryon scaling near the QCD critical point

N.G. Antoniou<sup>1</sup>, F.K. Diakonov and A.S. Kapoyannis

*Department of Physics, University of Athens,  
GR-15771 Athens, Greece*

### Abstract

The net-baryon density at midrapidity is proposed as an order parameter in the search for the QCD critical point in heavy ion collisions. As a function of the initial energy and the total number of participants, this quantity obeys a scaling law, dictated by the critical exponents of the appropriate universality class. The corresponding scaling variable specifies the proximity of a given experiment to the critical point. Within this framework, measurements at the SPS are discussed and predictions for RHIC and LHC are extracted.

---

<sup>1</sup>e-mail: nantonio@cc.uoa.gr

# 1 Introduction

A remarkable property of the QCD phase diagram ( $\rho - T$ ) is the existence of an endpoint along the critical line of the first order quark-hadron phase transition [1]. It defines a critical point of second order, belonging to the universality class of a  $3d$  Ising system and located on a line of nonzero baryonic density  $\rho = \rho_c$ . The QCD critical point is associated with the chiral phase transition in the sense that it is the remnant of a tricritical point corresponding to the chiral limit  $m_u = m_d = 0$  [2]. In other words, the existence of a second-order critical point, at nonzero baryonic density, is a fundamental property of real QCD with small but nonzero quark masses ( $m_u, m_d \neq 0$ ). The QCD critical point communicates with the hadronic world through the fluctuations of a scalar field ( $\sigma$ -field) which carries the quantum numbers of an isoscalar ( $\sigma$ -meson) as the manifestation of a quark condensate,  $\sigma \sim \langle \bar{q}q \rangle$ , in thermal environment. At the critical temperature (and infinite volume) the isoscalar has zero mass, in order to provide the infinite wavelength mode required by the divergence of the correlation length. It remains, therefore, stable in the thermal environment of a nuclear collision as long as the temperature stays close to the critical value. At the freeze-out stage the mass of the  $\sigma$ -field may reach the two-pion threshold ( $m_\sigma \gtrsim 2m_\pi$ ) and become accessible to observation [2, 3]. In the effective theory of the QCD critical point, the classical  $\sigma$ -field is a natural order parameter, the fluctuations of which obey scaling laws dictated by the critical exponents of the  $3d$  Ising system ( $\eta \approx 0, \beta \approx \frac{1}{3}, \delta \approx 5, \nu \approx \frac{2}{3}$ ). In a baryonic environment, however, the chiral condensate is expected to have, at  $T = T_c$ , a strong dependence on the net-baryon density, driving the  $\sigma$ -field close to zero for  $\rho \approx \rho_c$ :  $\langle \bar{q}q \rangle_\rho \approx \lambda \left( \frac{\rho - \rho_c}{\rho_c} \right) \langle \bar{q}q \rangle_0 + O[(\rho - \rho_c)^2]$  where  $\lambda$  is a dimensionless constant of the order of unity [4]. This dependence suggests a new order parameter,  $m = \rho - \rho_c$ , associated with the critical properties of the baryonic fluid created in a quark-hadron phase transition. In fact, approaching the critical point in the phase diagram, both the  $\sigma$ -field fluctuations and the fluctuations of the order parameter  $m(\vec{x})$  obey the same scaling laws ( $\langle \bar{q}q \rangle_\rho \sim m(\vec{x})$ ).

In this work we exploit the scaling properties of the order parameter  $m(\vec{x})$ , properly adjusted to measurable quantities, in heavy ion collisions. For this purpose we consider net-baryon production in collisions of heavy nuclei with total number of participants  $A_t$  and initial energy corresponding to a total size in rapidity  $\Delta y = L$ . The paper is organized as follows: In Section 2 we discuss in detail the scaling properties of the net-baryon fluid

near the critical point. In Section 3 we present shortly phenomenological consequences of the presence of critical fluctuations in the baryonic sector. Finally in Section 4 we present our conclusions concerning the possibility to approach and observe the QCD critical point in heavy-ion colliders.

## 2 Net-baryon scaling

The created baryons in the process of quark-hadron phase transition occupy a cylindrical volume with transverse radius  $R_{\perp} \sim A_{\perp}^{1/3}$  and longitudinal size  $L$  (in rapidity). The parameter  $A_{\perp}$  specifies the effective number of participants, contributing to the transverse geometry of the collision, and it is assumed  $A_{\perp} \approx \frac{A_t}{2}$ , valid both for central ( $A_{\perp} = A_{min}$ ) and non-central collisions. Projecting out the net-baryon system onto the longitudinal direction we end up with a  $1d$  liquid confined in a finite rapidity region of size  $L$  with local density  $\rho(y) = \frac{n_b(y)}{\pi R_{\perp}^2 \tau_f}$ , directly related to the measurable net-baryon density in rapidity  $n_b(y) = \frac{dN_b}{dy}$ . Putting  $R_{\perp} = R_o A_{\perp}^{1/3}$ , we introduce a characteristic volume  $V_o = \pi R_o^2 \tau_f$  in terms of the freeze-out time scale  $\tau_f \geq 6 - 8 fm$  [5] and the nuclear-size scale  $R_o$  which contains also any growth effects near the critical point ( $R_o \geq 1.2 fm$ ). Using  $V_o^{-1}$  as a scale for baryonic, freeze-out densities, the order parameter  $m(y)$  of the  $1d$  baryonic liquid is written:

$$m(y) = A_{\perp}^{-2/3} n_b(y) - \rho_c \quad , \quad 0 \leq y \leq L \quad (1)$$

In what follows, our basic assumption is that the deconfined phase of quark matter, in heavy-ion collisions, approaches the QCD critical point in local thermal equilibrium. In the framework of inside-outside mechanism, this process is implemented by considering the isothermal space-time hyperbolas  $t^2 - x_{\parallel}^2 = \tau^2$  and employing the corresponding rapidity variable as the appropriate longitudinal coordinate. In this description, the assumed local equilibrium in the conventional geometry  $(x_{\parallel}, \vec{x}_{\perp}, t)$  is translated as global equilibrium in the new geometry  $(y, \vec{x}_{\perp}, \tau)$  and one may consistently impose, near criticality, static scaling laws on the order parameter  $m(y)$ . In particular, the expected singularity at  $T = T_c$  is incorporated in a general expansion of the form:

$$m(y) = t^{\beta} [F_o(y/L) + tF_1(y/L) + \dots] \quad (2)$$

where  $t \equiv \frac{T_c - T}{T_c}$  and  $\beta$  is the appropriate critical exponent ( $\beta \approx \frac{1}{3}$ ). The leading term  $F_o(y/L)$  in the expansion (2) has a universal power-law behaviour near the walls ( $y = 0, L$ ), shared by all fluids belonging to the same universality class and confined in a finite, one-dimensional region [6, 7]. At midrapidity ( $y \approx \frac{L}{2}$ ), eq.(2) gives the deviation of the measurable, bulk density of net baryons, from the critical value  $\rho_c$ , as we approach the critical point, not along the critical isochore ( $\rho = \rho_c$ ) but along the freeze-out line:

$$A_{\perp}^{-2/3} n_b = \rho_c + t_f^{\beta} [F_o + t_f F_1 + \dots] \quad (3)$$

where  $t_f = \frac{T_c - T_f}{T_c}$ ,  $n_b = n_b(L/2)$ ,  $F_i = F_i(1/2)$  and  $T_f$  is the freeze-out temperature. Integrating now eq.(2) in the interval  $0 \leq y \leq L$  we obtain at  $T = T_f$ :

$$A_{\perp}^{-2/3} A_t L^{-1} = \rho_c + t_f^{\beta} (I_o + t_f I_1 + \dots) \quad (4)$$

where  $I_i = \int_0^1 F_i(\xi) d\xi$ . Introducing the variable  $z_c = A_{\perp}^{-2/3} A_t L^{-1}$  we find from eqs.(3) and (4) a scaling law for the net-baryon density at midrapidity:

$$A_{\perp}^{-2/3} n_b = \Psi(z_c, \rho_c) \quad ; \quad z_c \geq \rho_c \quad (5)$$

where the scaling function  $\Psi(z_c, \rho_c)$  has the property  $\Psi(z_c = \rho_c, \rho_c) = \rho_c$ . In the crossover regime  $z_c < \rho_c$ , where critical fluctuations disappear, the local density at midrapidity is, to a good approximation,  $n_b \approx A_t L^{-1}$  suggesting a continuous extension of the scaling law (5) in this region with  $\Psi(z_c, \rho_c) = z_c$  ( $z_c < \rho_c$ ). It is of interest to note that although the scaling function  $\Psi(z_c, \rho_c)$  is continuous at the critical point ( $z_c = \rho_c$ ), the first derivative is expected to be discontinuous at this point in accordance with the nature of the phase transition (critical point of second order).

In order to study in detail the critical behaviour of the baryonic fluid in terms of the new variables  $n_b, z_c$  a further investigation of the structure of the scaling function  $\Psi(z_c, \rho_c)$  for  $z_c \geq \rho_c$  is necessary. For this purpose we approximate the nearby part of the freeze-out line, close to the critical point ( $t_f \ll 1$ ), by truncating the series (2) keeping only the next to the leading term  $F_1(y/L)$ . As a result, the equations (3) and (4) are written correspondingly:

$$A_{\perp}^{-2/3} n_b \approx \rho_c + t_f^{\beta} (F_o + t_f F_1) \quad (6-a)$$

$$z_c - \rho_c \approx t_f^{\beta} (I_o + t_f I_1) \quad (6-b)$$

Neglecting terms of order  $O(t_f^2)$  in the power expansion of the quantity  $(I_o + t_f I_1)^{1/\beta}$  and combining eqs.(6) we finally obtain:

$$A_{\perp}^{-2/3} n_b = \rho_c + \frac{F_o}{F_1} [f(z_c, \rho_c)]^{\beta} + C [f(z_c, \rho_c)]^{\beta+1} \quad (7-a)$$

$$A_{\perp}^{-2/3} n_b = \rho_c + F_o t_f^{\beta} \left(1 + t_f \frac{C I_o^{1+\frac{1}{\beta}}}{F_o}\right) \quad (7-b)$$

$$f(z_c, \rho_c) = \frac{1}{G} \left(-1 + \sqrt{1 + 2G(z_c - \rho_c)^{1/\beta}}\right) \quad ; \quad z_c \geq \rho_c \quad (7-c)$$

where  $C = \frac{F_1}{I_o^{1+\frac{1}{\beta}}}$ ,  $G = \frac{2I_1}{\beta I_o^{1+\frac{1}{\beta}}}$ .

The component  $F_o(y/L)$  which dominates the order parameter  $m(y)$  in the limit  $T \rightarrow T_c$  is approximately constant in the central region ( $y \approx \frac{L}{2}$ ,  $L \gg 1$ ), far from the walls (at the points  $y = 0, L$ ) due to the approximate translational invariance of the finite system in this region. On the other hand, approaching the walls,  $F_o(y/L)$  describes the density correlation with the endpoints and obeys a universal power law. In summary:

$$F_o(\xi) \sim \text{const.} \quad \left(\xi \approx \frac{1}{2}\right) \quad (8-a)$$

$$F_o(\xi) \sim \xi^{-\beta/\nu} \quad (\xi \geq 0) \quad (8-b)$$

$$F_o(\xi) \sim (1 - \xi)^{-\beta/\nu} \quad (\xi \leq 1) \quad (8-c)$$

The solution which fulfils these requirements is:

$$F_o(\xi) = g[\xi(1 - \xi)]^{-\beta/\nu} \quad (0 \leq \xi \leq 1) \quad (9-a)$$

$$\frac{F_o}{I_o} = \frac{4^{\beta/\nu}}{B\left(1 - \frac{\beta}{\nu}, 1 - \frac{\beta}{\nu}\right)} \quad ; \quad B(n, m) = \frac{\Gamma(m)\Gamma(n)}{\Gamma(m+n)} \quad (9-b)$$

Inserting the constant  $\frac{F_o}{I_o}$  into the eq.(7-b), the final form of the scaling function  $\Psi(z_c, \rho_c)$  is obtained:

$$\begin{aligned} \Psi(z_c, \rho_c) &= \rho_c + \frac{4^{\beta/\nu}}{B\left(1 - \frac{\beta}{\nu}, 1 - \frac{\beta}{\nu}\right)} [f(z_c, \rho_c)]^{\beta} \\ &\quad + C [f(z_c, \rho_c)]^{\beta+1} \quad ; \quad z_c \geq \rho_c \end{aligned} \quad (10-a)$$

$$\Psi(z_c, \rho_c) = z_c \quad ; \quad z_c < \rho_c \quad (10-b)$$

where  $f(z_c, \rho_c)$  is given by eq.(7-c). It is straightforward to show that the discontinuity of the first derivative of  $\Psi(z_c, \rho_c)$  at  $z_c = \rho_c$  is a nonzero universal

constant:  $disc\left(\frac{d\Psi}{dz_c}\right)_{\rho_c} \approx 1 - \frac{2}{\pi} \left(\frac{\beta}{\nu} \approx \frac{1}{2}\right)$  as expected from the characteristic properties of a second-order phase transition. Combining eqs.(5-10) one may propose a framework for the treatment of certain phenomenological aspects of the QCD critical point. The scaling law (5) combined with eq.(10) involves three nonuniversal parameters: (a) the critical density  $\rho_c$  and (b) the constants  $C, G$  which give a measure of the nonleading effects, allowing to accomodate in the scaling function (10) processes not very close to the critical point. We have used measurements at the SPS in order to fix these parameters on the basis of eqs.(5) and (10). More specifically, in a series of experiments (Pb+Pb, S+Au, S+Ag, S+S) with central and noncentral (Pb+Pb) collisions at the SPS [8, 9] net baryons have been measured at midrapidity whereas the scaling variable  $z_c = A_{\perp}^{-2/3} A_t L^{-1}$ , associated with these experiments, covers a sufficiently wide range of values ( $1 \leq z_c \leq 2$ ) allowing for a best fit solution. The outcome of the fit is consistent with the choice  $G \approx 0$  and the equations (7) are simplified as follows:

$$A_{\perp}^{-2/3} n_b = \rho_c + \frac{2}{\pi}(z_c - \rho_c) + C(z_c - \rho_c)^4 \quad (11-a)$$

$$A_{\perp}^{-2/3} n_b = \rho_c + \frac{2I_o}{\pi} t_f^{1/3} \left(1 + t_f \frac{\pi C I_o^{1/3}}{2}\right) \quad (11-b)$$

$$A_{\perp}^{-2/3} n_b(y) = \rho_c + \frac{(z_c - \rho_c)L}{\pi\sqrt{y(L-y)}} + O[(z_c - \rho_c)^4] \quad (11-c)$$

In eqs.(11) we have used the approximate values of the critical exponents  $\beta \approx \frac{1}{3}$ ,  $\frac{\beta}{\nu} \approx \frac{1}{2}$  in the  $3d$  Ising universality class [10]. We have also added eq.(11-c) which gives the universal behaviour of the net-baryon density  $n_b(y)$ , in the vicinity of the critical point ( $z_c - \rho_c \ll 1$ ). The fitted values of the parameters in eq.(11-b) are  $\rho_c = 0.81$ ,  $C = 0.68$  and the overall behaviour of the solution is shown in Fig. 1. It turns out that the critical density is rather small, compared to the normal nuclear density  $\rho_o \approx 0.17 \text{ fm}^{-3}$ :  $\rho_c \leq \frac{\rho_o}{5}$  ( $R_o \geq 1.2 \text{ fm}$ ,  $\tau_f \geq 6 \text{ fm}$ ), suggesting that the critical temperature remains close to the value  $T_c \approx 140 \text{ MeV}$  obtained in studies of QCD on the lattice at zero chemical potential [11]. The difference  $d_c = |z_c - \rho_c|$  in Fig. 1 is a measure of the proximity of a given experiment ( $A_t, L$ ) to the critical point. We observe that the central Pb+Pb collisions at the SPS ( $d_c \approx 1.1$ ) drive the system into the most distant freeze-out area, from the critical point, as compared to other processes at the same energy. In fact, the most suitable experiments to bring quark matter close to the critical point at the SPS are:

S+S ( $d_c \approx 0.18$ ), S<sub>i</sub>+S<sub>i</sub> ( $d_c \approx 0.20$ ) and C+C ( $d_c \approx 0.06$ ), central collisions. One may even reach the critical point ( $d_c \approx 0$ ) at the SPS with medium-size nuclei, either in noncentral collisions: S+S, S<sub>i</sub>+S<sub>i</sub> ( $A_t \approx 29$ ) or at lower energies: C+C ( $P \approx 130 A \frac{GeV}{c}$ ). Also, the experiments at RHIC, with central Au+Au ( $d_c \approx 0.27$ ) collisions, come close to the critical point and may even reach it exactly ( $d_c \approx 0$ ) either with lighter nuclei or with noncentral Au+Au collisions ( $A_t \approx 165$ ). Finally at the LHC ( $\sqrt{s} \approx 5.5 TeV$ ), Pb+Pb collisions are expected to drive quark matter into the crossover area ( $z_c < \rho_c$ ,  $d_c \approx 0.13$ ) where no critical fluctuations occur. At lower energies however ( $\sqrt{s} \approx 1.4 TeV$ ), Pb+Pb central collisions may reach the critical point even at the LHC. Obviously, in order to have a clear answer on the proximity of a given experiment to the critical point, precision measurements of the net-baryon density at midrapidity, in a wide range of energies (between SPS and RHIC), are needed, both for central and noncentral collisions. With such measurements, the scaling law (5) may be tested in its full extent and a sharp determination of the critical density can be achieved through eq.(7a).

The freeze-out line ( $n_b$  versus  $T_f$ ) given by eq.(11b) is shown in Fig. 2. We have used the freeze-out temperatures for the processes [12]: Pb+Pb ( $T_f \approx 115 MeV$ ) and S+S ( $T_f \approx 145 MeV$ ) at the SPS, in order to determine the critical temperature,  $T_c \approx 145 MeV$ , and fix the parameter  $I_o \approx 1.86$ . Again, we notice that the relatively small value of the freeze-out temperature in Pb+Pb collisions (at the SPS) is associated with the fact that in this process the system of quark matter is not driven close to the critical point. On the contrary the freeze-out temperature in S+S collisions remains practically equal to the critical value, due to the proximity of this process to the critical point, at the freeze-out stage (Fig. 1). Finally, in Fig. 3, the rapidity distribution of net baryons in Au+Au collisions at RHIC ( $L \approx 11, z_c \approx 1.1$ ) is shown, relying upon the fact that in this process the distance from the critical point is small ( $d_c \approx 0.27$ ) and eq.(11-c) is valid.

### 3 Baryonic critical fluctuations

Once the phase of quark matter has reached the critical point in a particular class of experiments, as discussed in the previous section, strong critical fluctuations are expected to form intermittency patterns both in the pion and net-baryon sector. As already mentioned in the introduction, the origin of these fluctuations can be traced in the presence, at  $T = T_c$ , of a zero mass

field with a classical profile ( $\sigma$ -field) which, under the assumption of a phase transition in local thermal equilibrium, is described by an effective action in  $3 - d$ , the projection of which onto rapidity space is written as follows [3]:

$$\Gamma_c \approx \frac{\pi R_\perp^2}{C_A} \int_{\delta y} dy \left[ \frac{1}{2} \left( \frac{\partial \sigma}{\partial y} \right)^2 + 2C_A^2 \beta_c^4 \sigma^{\delta+1} \right] \quad ; \quad C_A = \frac{\tau_c}{\beta_c}, \quad \beta_c = T_c^{-1} \quad (12)$$

Equation (12) gives the free energy of the  $\sigma$ -field within a cluster of size  $\delta y$  in rapidity and  $R_\perp$  in transverse space. The critical fluctuations generated by (12) in the pion sector have been studied extensively in our previous work [3], therefore, in what follows, we are going to discuss the fluctuations induced by the  $\sigma$ -field in the net-baryon sector, noting that a direct measurement of these fluctuations may become feasible in current and future heavy-ion experiments. For this purpose we introduce in eq.(12) the order parameter  $m(y)$  through the following equations:

$$\begin{aligned} \sigma(y) &\approx F \beta_c^2 m(y) \quad ; \quad F \equiv -\frac{\lambda \langle \bar{q}q \rangle_o}{\rho_c} \quad ; \quad \langle \bar{q}q \rangle_o \approx -3 f m^{-3} \\ \Gamma_c &\approx g_1 \int_{\delta y} dy \left[ \frac{1}{2} \left( \frac{\partial \hat{m}}{\partial y} \right)^2 + g_2 |\hat{m}|^{\delta+1} \right] \quad ; \quad \hat{m}(y) = \beta_c^3 m(y) \end{aligned} \quad (13)$$

where:  $g_1 = F^2 \left( \frac{\pi R_\perp}{C_A \beta_c^2} \right)$ ,  $g_2 = 2C_A^2 F^4$ . The partition function  $Z = \int \mathcal{D}[\hat{m}] e^{-\Gamma_c[\hat{m}]}$  for each cluster is saturated by instanton-like configurations [13] which for  $\delta y \leq \delta_c$  lead to self-similar structures, characterized by a pair-correlation function of the form:

$$\langle \hat{m}(y) \hat{m}(0) \rangle \approx \frac{5}{6} \frac{\Gamma(1/3)}{\Gamma(1/6)} \left( \frac{\pi R_\perp^2 C_A}{\beta_c^2} \right) F^{-1} y^{-\frac{1}{\delta+1}} \quad (14)$$

The size, in rapidity, of these fractal clusters is  $\delta_c \approx \left( \frac{\pi R_\perp^2}{16 \beta_c^2 C_A^2} \right)^{2/3}$  according to the geometrical description of the critical systems [13]. Integrating eq.(14) we find the fluctuation  $\langle \delta n_b \rangle$  of the net-baryon multiplicity with respect to the critical occupation number within each cluster, as follows:

$$\langle \delta n_b \rangle \approx F^{-1} \left( \frac{\pi R_\perp^2 C_A}{2 \beta_c^2} \right) \frac{2^{2/3} \Gamma(1/3)}{\Gamma(1/6)} \delta_c^{5/6} \quad (15)$$



The dimensionless parameter  $F$  is of the order  $10^2$  and the size  $\delta_c$ , on general grounds ( $R_\perp \lesssim 2\tau_c$ ) is of the order of one ( $\delta_c \lesssim 1$ ). This is in agreement with the fact that the rapidity separation of two causally correlated space-time events is logarithmically bounded,  $\delta y \leq \ln\left(1 + \frac{\delta\tau_c}{\tau_c}\right)$ , leading, practically, to a direct correlation length of the order of one ( $\delta y \lesssim 1$ ). However, in reality, the global baryonic system develops fluctuations at all scales in rapidity since the direct correlation ( $O(\delta_c)$ ) propagates along the entire system through the cooperation of many self-similar clusters of relatively small size ( $\delta_c \approx 0.35$  and  $\langle \delta n_b \rangle \approx 140$ ). We have quantified this mechanism in a Monte-Carlo simulation for the conditions of the experiments at RHIC (in RHIC the size of the system is  $L \approx 11$ ) in order to generate baryons with critical fluctuations. The distribution of the order parameter  $|m(y)|$  describing the fluctuations of the “critical” baryons in the rapidity space for a typical event as well as the corresponding intermittency analysis in terms of factorial moments are presented in Fig. 4. The intermittency exponent of the second moment  $F_2$  in rapidity is found to be  $s_2 \approx 0.18$  which is very close to the theoretically expected value ( $\frac{1}{6}$ ) of a monofractal  $1 - d$  set with fractal dimension  $\frac{5}{6}$ . The quantitative details of this new class of phenomena, concerning critical fluctuations in the net-baryon sector, and in particular the intermittency pattern of the observable net-baryon density, go beyond the purpose of this Letter and will be presented elsewhere [14].

## 4 Concluding remarks

In conclusion, we have shown that the baryonic sector in an experiment with heavy ions, possess valuable information regarding the proximity and observation of the second order QCD critical point. Complementary suggestions for the significance of net-baryon fluctuations in order to trace the critical line of first order in the phase diagram are described in [16]. In particular the measurements of net-baryon spectra in rapidity provide a valuable set of observables in heavy ion experiments, in connection with the phenomenology of the QCD critical point. The trend of the existing data at the SPS suggests the presence of a critical point of second order in the phase diagram (Figs. 1,2) specified by the critical values of temperature and density:  $T_c \approx 145 \text{ MeV}$ ,  $\rho_c \leq \frac{\rho_0}{5}$ . A scaling law for the net-baryon density at midrapidity  $n_b$ , as a function of the initial energy and the number of participants, has been established in the neighbourhood of the critical point. The scaling function

incorporates the indices of the universality class (critical exponents) whereas the scaling variable gives a measure of the proximity of a given experiment to the critical point. On the basis of this investigation, the experiments at RHIC are very likely to reach the QCD critical point and as a first sign of this new phenomenon we have predicted a rather unconventional profile of net-baryon density in rapidity (in Au+Au collisions), associated with the presence of a critical point, nearby (Fig. 3). Finally we have indicated the presence of strong intermittency effects in the rapidity spectrum of the net baryons which can in principle be used to reveal experimentally the QCD critical point and confirm its universality class (Fig. 4).

## References

- [1] F. Wilczek, hep-ph/0003183.
- [2] M. Stephanov, K. Rajagopal and E. Shuryak, Phys. Rev. Lett. **81**, 4816 (1998); J. Berges, D.-U. Jungnickel and C. Wetterich, Phys. Rev. D59 (1999) 034010; Eur. Phys. J. C13 (2000) 323.
- [3] N.G. Antoniou, Y.F. Contoyiannis and F.K. Diakonou, Nucl. Phys. **A661**, 399c (1999).
- [4] R. Brockmann and W. Weise, Phys. Lett. **B367**, 40 (1996).
- [5] B. Müller, Nucl. Phys. **A661**, 272c (1999).
- [6] A. Maciolek, R. Evans and C. R. Wilding, Phys. Rev. **E60**, 7105 (1999).
- [7] M.E. Fisher and P.G. de Gennes, C.R. Seances Acad. Sci. **B287**, 207 (1978).
- [8] The NA35 Collaboration, Eur. Phys. J. **C2**, 634 (1998); D. Röhrich (NA35 Collaboration), Nucl. Phys. **A566**, 35c (1994); F. Siklér (NA49 Collaboration), Nucl. Phys. **A661**, 45c (1999).
- [9] G.E. Cooper (NA49 Collaboration), Nucl. Phys. **A661**, 362c (1999).
- [10] S.K. Ma, *Modern Theory of Critical Phenomena*, (Benjamin/Cummings, Reading, MA, 1976).

- [11] E. Laermann, Nucl. Phys. **A610**, 1c (1996).
- [12] V. Heinz, J. Phys. **G25**, 263 (1999); R. Stock, Nucl. Phys. **A661**, 282c (1999).
- [13] N.G. Antoniou, Y.F. Contoyiannis, F.K. Diakonov and C.G. Papadopoulos, Phys. Rev. Lett. **81**, 4289 (1998); N.G. Antoniou, Y.F. Contoyiannis and F.K. Diakonov, Phys. Rev. **62E**, 3125 (2000).
- [14] N.G. Antoniou, F.K. Diakonov and A.S. Kapoyannis (in preparation).
- [15] A. Bialas and R. Peschanski, Nucl. Phys. **B273**, 703 (1986); **B308** 857 (1988).
- [16] S. Gavin, nucl-th/9908070.

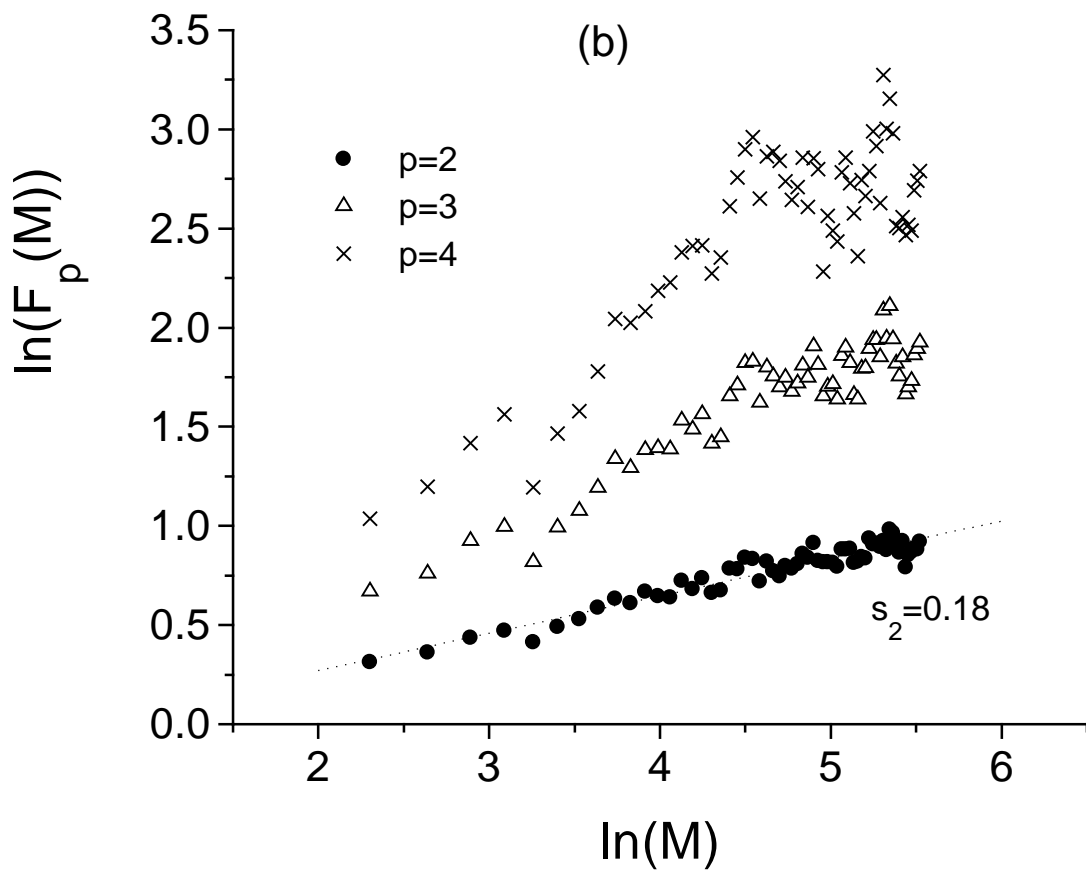
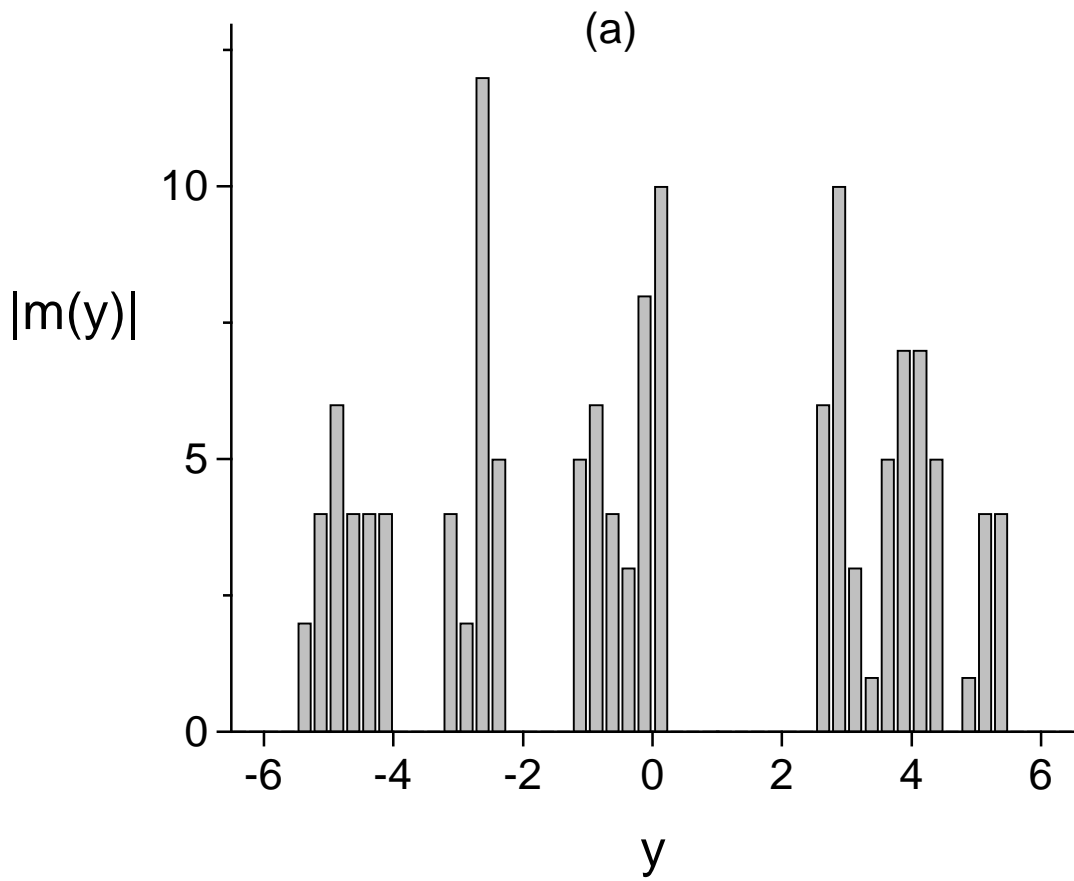
### Figure Captions

FIG. 1. The scaling law (10) is illustrated together with measurements at the SPS. The critical point and the corresponding break in the slope of  $\Psi(z_c, \rho_c)$  are also shown.

FIG. 2. The freeze-out line,  $n_b$  as a function of  $t_f$ , is illustrated together with measurements at the SPS (S+S, Pb+Pb). The extracted freeze-out points for S+Au and S+Ag are also shown in this diagram.

FIG. 3. The net-baryon profile in rapidity for Au+Au collisions at RHIC energies is shown, as predicted by eq.(11-c).

FIG. 4. (a) The distribution of  $|m(y)|$  in rapidity for a MC-generated event. (b) The first three factorial moments for the event shown in (a) in a log-log plot. A linear fit determining the slope  $s_2$  ( $\approx 0.18$ ) of the second moment is also shown.



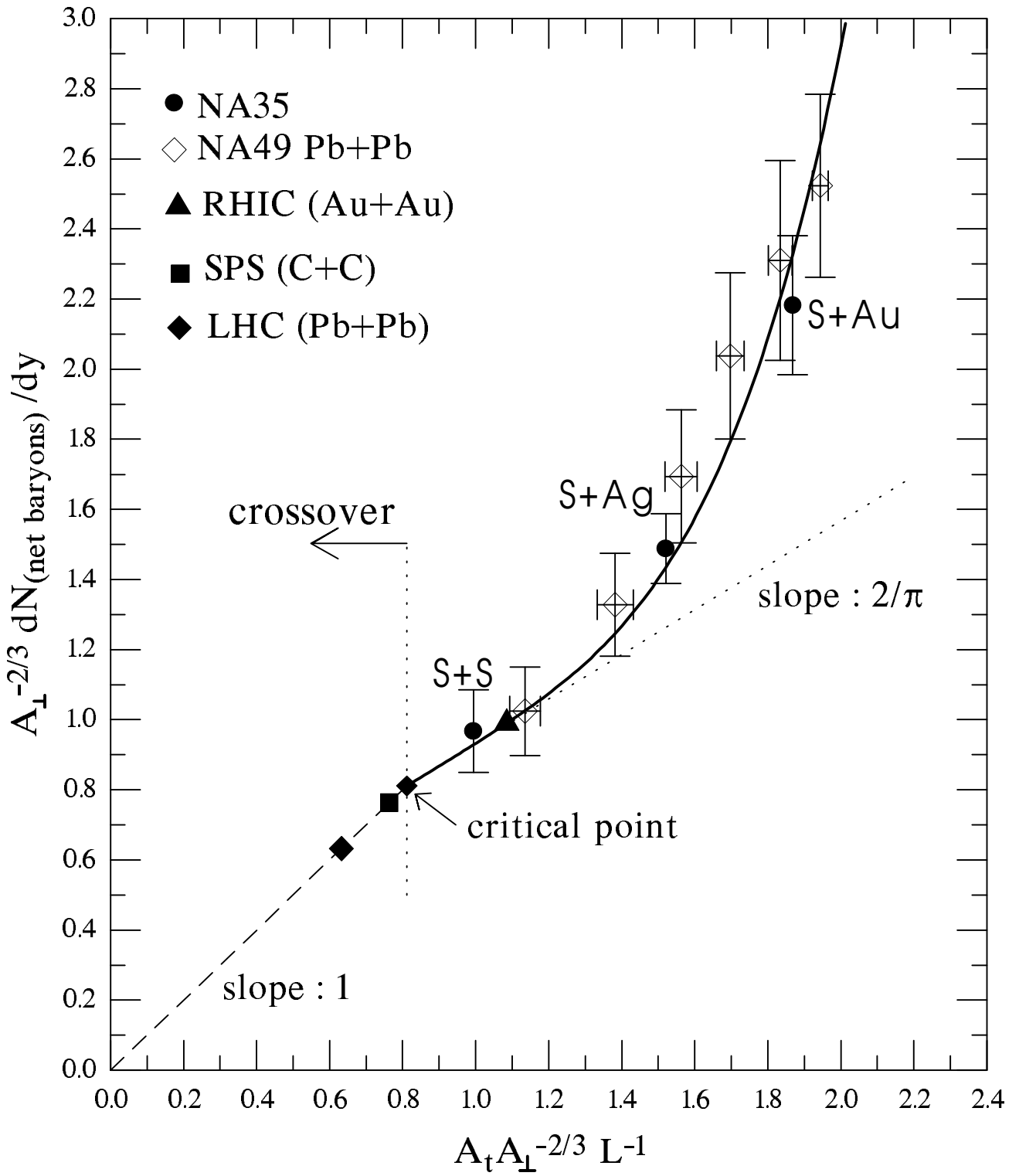


Fig. 1

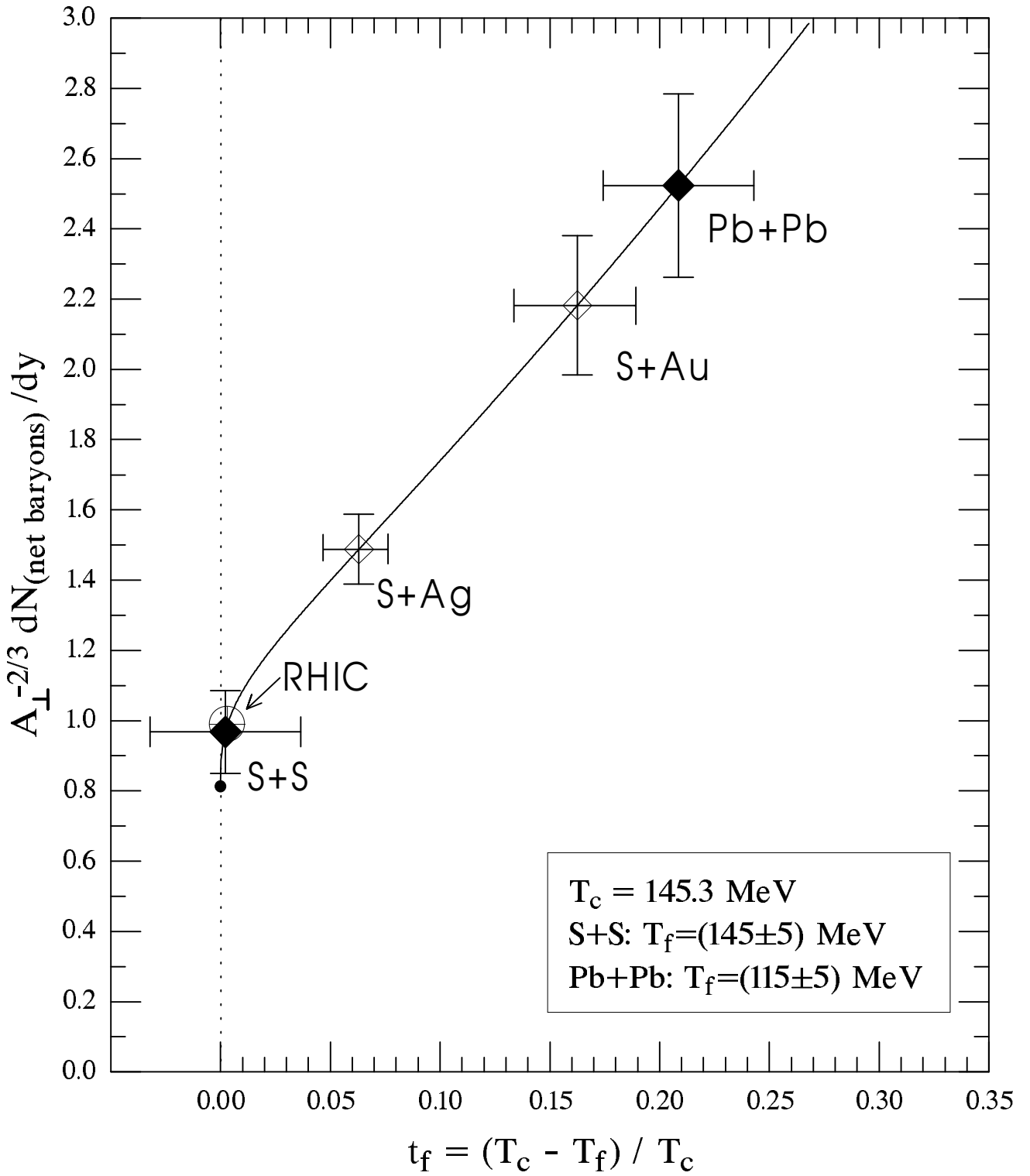


Fig. 2

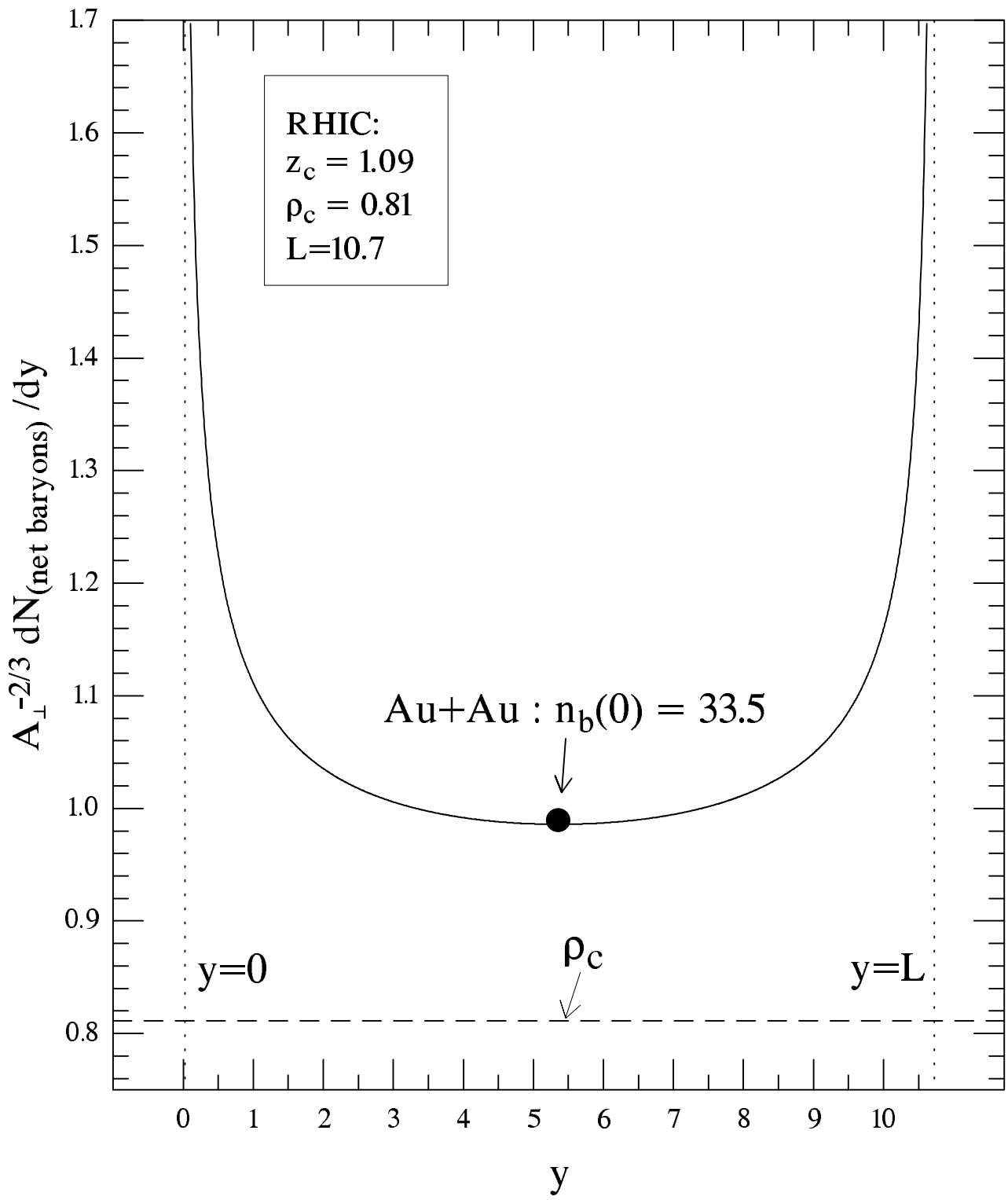


Fig. 3